

**Exact counterdiabatic driving in finite topological lattice models**Callum W. Duncan <sup>\*</sup>*Department of Physics and SUPA, University of Strathclyde, Glasgow G4 0NG, United Kingdom*

(Received 27 March 2024; revised 15 May 2024; accepted 5 June 2024; published 18 June 2024)

Adiabatic protocols are often employed in state preparation schemes but require the system to be driven by a slowly varying Hamiltonian so that transitions between instantaneous eigenstates are exponentially suppressed. Counterdiabatic driving is a technique to speed up adiabatic protocols by including additional terms calculated from the instantaneous eigenstates that counter diabolic excitations. However, this approach requires knowledge of the full eigenspectrum meaning that the exact analytical form of counterdiabatic driving is only known for a subset of problems, e.g., the harmonic oscillator and transverse field Ising model. We extend this subset of problems to include the general family of one-dimensional noninteracting lattice models with open boundary conditions and arbitrary onsite potential, tunneling terms, and lattice size. We will derive a general analytical form for the counterdiabatic term for all states of lattice models, including bound and in-gap states which appear, e.g., in topological insulators. We also derive the general analytical form of targeted counterdiabatic driving terms which are tailored to enforce the dynamical state to remain in a specific state. As an example of the use of the derived analytical forms, we consider state transfer using the topological edge states of the Su-Schrieffer-Heeger model. The derived analytical counterdiabatic driving Hamiltonian can be utilized to inform control protocols in many-body lattice models or to probe the nonequilibrium properties of lattice models.

DOI: [10.1103/PhysRevB.109.245421](https://doi.org/10.1103/PhysRevB.109.245421)**I. INTRODUCTION**

The adiabatic approximation is utilized to enable a variety of aspects of quantum science. This includes state preparation, the paradigm of adiabatic quantum computing [1,2], and coherent quantum annealing [3,4]. It states that if we initiate a system in an eigenstate of its Hamiltonian, then the dynamical solution to the Schrödinger equation as we change a parameter in said Hamiltonian, will approximately remain in the corresponding instantaneous eigenstate up to a phase factor [5,6]. This approximation relies upon the parameter changing slowly, as it is natural in such a scenario to describe the dynamical state entirely in the adiabatic basis of the instantaneous eigenstates of the changing Hamiltonian. If the state remains nondegenerate and the gap between it and all other states is large with respect to the inverse of the time taken to traverse the energy landscape, then the adiabatic approximation is valid [7]. This makes the adiabatic approximation difficult to realize if the parameter change includes the crossing of a phase transition or, as we will see below, the closing of a band gap. In any finite time protocol, there will always be a nonzero probability of transitioning to other states, and this is exasperated in most experimental settings due to the limited time allocated to an adiabatic protocol

as well as losses, heating, noise, and dissipation. Therefore, speeding up adiabatic protocols, or finding alternative state preparation schemes, is crucial.

There are many approaches to the particular problem of speeding up an adiabatic protocol, including numerical optimal control [8,9] and shortcuts to adiabaticity [10,11]. In this work, we will extend the analytical approach of counterdiabatic driving (CD) to include the general family of Hamiltonians of noninteracting particles in one-dimensional (1D) lattices. CD was first introduced by Demirplak and Rice [12,13] in quantum chemistry before being independently introduced as transitionless driving by Berry [14]. CD adds control terms to the dynamical Hamiltonian such that the adiabatic approximation is enforced as the solution of the dynamical Schrödinger equation for all timescales. It is found that by solving for the instantaneous eigenstates at all times, such a control term can be constructed and we will go through this in detail in Sec. II. Due to CD's reliance on knowledge of the instantaneous eigenstates, its exact form is only known for a very limited set of problems, e.g., harmonic oscillators [15] and the integrable transverse Ising model [16,17], to which we will add noninteracting lattice models.

For a broader context, we note that approaches have been developed to give approximate CD terms for complex settings where it is not possible to construct the exact CD, with the most successful to date being that of local, or variational, CD [18–20]. This approach relies on recasting the CD terms into a description in terms of the adiabatic gauge potential, which encodes all of the diabatic transitions that one needs to counter and is equivalent to the CD term we will define in Sec. II. An approximation to the adiabatic gauge potential is then obtained through a variational minimization procedure. The

<sup>\*</sup>Contact author: [callum.duncan@strath.ac.uk](mailto:callum.duncan@strath.ac.uk)

case of noninteracting particles in 1D lattices was considered as an example in the original proposal for local CD [18] and an approximate adiabatic gauge potential was obtained. The approach of local CD has been further developed to include its combination with numerical optimal control to improve annealing protocols [21] and to inform the structure of terms utilized in reinforcement learning for optimal control [22]. Local CD has been implemented experimentally for adiabatic state transfer in a one-dimensional lattice [23] and has been extended to many-body lattice models [24,25]. Recently, numerical approaches to derive the adiabatic gauge potential in general many-body settings have been introduced either utilizing Krylov subspace methods [26] or the Lie algebra of the expansion [27].

While the methods presented in this work can be applied to any general noninteracting 1D lattice model, we will focus on the particularly interesting case of time-reversal-symmetric topological insulators which can host edge modes in the band gaps of their spectrum [28–31]. While direct brute-force numerical diagonalization of the time-independent Schrödinger equation is always an option, analytical approaches have been developed to characterize the topological states in cases of semi-infinite commensurate lattices [32,33] through the extension of Bloch’s theorem. It is also possible to obtain the topological edge states from the bound states of scattering matrix approaches [34,35]. We will utilize the approach of Ref. [36], which allows for all states to be obtained, both within energy bands and in the gaps between them, for general 1D noninteracting topological lattice models with open boundary conditions. We will outline this approach in Sec. III which will enable us to write the general analytical form of CD for noninteracting lattice models in Sec. IV. We will then consider as an example the topological Su-Schrieffer-Heeger (SSH) model which has been used as a toy model for the control of topologically protected state transfer protocols [37–45]. We will show both the form of the analytically obtained CD for the SSH model and consider the properties of the modified dynamical Hamiltonian which enforces adiabaticity.

## II. COUNTERDIABATIC DRIVING

CD enforces the adiabatic approximation to be the dynamical solution to Schrödinger’s equation through the addition of control terms [12–14]. For an arbitrary time-dependent Hamiltonian  $H[\lambda(t)]$ , where  $\lambda(t)$  is the changing parameter, the instantaneous eigenstates  $|\psi_n[\lambda(t)]\rangle$  and energies  $E_n[\lambda(t)]$  are given by

$$H[\lambda(t)]|\psi_n[\lambda(t)]\rangle = E_n[\lambda(t)]|\psi_n[\lambda(t)]\rangle, \quad (1)$$

with  $n$  being the quantum number of the eigenstates. The adiabatic approximation then gives the solution of the dynamical Schrödinger’s equation to be

$$|\Psi_n[\lambda(t)]\rangle = \exp\left(-\frac{i}{\hbar} \int_{t_0}^{t_f} dt E_n[\lambda(t)]\right) |\psi_n[\lambda(t)]\rangle, \quad (2)$$

where we have excluded the Berry phase which would give the geometric phase in a cyclic protocol [46]. From here we

will drop the explicit time dependence of the parameter  $\lambda$  and work in units of  $\hbar = 1$ . We also note that the arguments of this section, and the rest of this work, can be easily extended to the case of a set of changing parameters.

To enforce Eq. (2) to be the solution to the dynamical Schrödinger equation in arbitrary driving times, we are required to add to the original Hamiltonian the CD term of [14]

$$H_{\text{CD}} = i \sum_n \dot{\lambda} |\partial_\lambda \psi_n(\lambda)\rangle \langle \psi_n(\lambda)|, \quad (3)$$

where  $\dot{\lambda}$  represents the derivative of the parameter  $\lambda$  with respect to time. In order to construct the exact CD term we therefore need to be able to solve the instantaneous Schrödinger equation for all points along the path dictated by  $\lambda$ .

## III. EXACT STATES OF NONINTERACTING LATTICE MODELS

We will briefly introduce the known solutions to the general noninteracting problem on a lattice described by the Hermitian Hamiltonian

$$H = \sum_{x=x_0+1}^{L-1} (-J_x b_x^\dagger b_{x+1} - J_x^* b_{x+1}^\dagger b_x + \mu_x n_x), \quad (4)$$

with the lattice being  $L$  sites labeled by  $x$  which takes consecutively increasing integer values between  $x_0 + 1$  and  $L - 1$ ,  $b_x^\dagger$  ( $b_x$ ) being the creation (annihilation) operator of a particle on the site at position  $x$ ,  $n_x$  the number operator on the site at  $x$ ,  $J_x$  the tunneling strength between sites  $x$  and  $x + 1$ , and  $\mu_x$  the onsite potential for site  $x$ . We will consider open boundary conditions and crystalline models where the system has a finite unit cell and thus a periodicity, which we label as  $\tau$ , allowing us to simplify the problem via Bloch’s theorem. However, the techniques outlined here can be applied in other one-dimensional lattice cases.

To obtain the analytical form of the counterdiabatic terms we will require that the system is described by Hamiltonian (4) and that we have open boundary conditions. We note that the solution could be obtained for periodic boundary conditions and on the infinite, or semi-infinite, lattice through the generalization of the results studied here, e.g., by using the states obtained in Refs. [32,33]. We will consider models with a repeated unit cell, and hence a periodicity, which is common to condensed matter problems. However, periodicity is not a required condition to analytically obtain the counterdiabatic driving terms corresponding to Hamiltonian (4), as the  $L$ -component Bloch function of an aperiodic model could, in principle, be solved for.

It may also be helpful to state what is not considered in this work. Primarily we note that the tight-binding model of Hamiltonian (4) does not allow for geometries beyond that of a one-dimensional chain, or for longer-range tunneling than nearest neighbors. We also do not consider terms due to interactions, with the common examples being onsite interactions and long-range interactions.

The noninteracting states which are solutions to the Schrödinger equation for Hamiltonian (4) can be written as

$$|\psi_\alpha\rangle = \sum_{x=x_0+1}^{L-1} \psi_\alpha(x) b_x^\dagger |0\rangle, \quad (5)$$

with  $|0\rangle$  being the state with no particles, and  $\psi_\alpha(x)$  being the coefficients of the state in each site  $x$ . We will refer to  $\psi_\alpha(x)$  as the wave function as it fully describes the quantum state. The general wave function for both states within a band or in a band gap, e.g., topological edge states [28,31] or Shockley-type bound states [47], can be written as [36]

$$\psi_\alpha(x) = N \left[ \phi_+(x) \alpha^x - \frac{\phi_+(L)}{\phi_-(L)} \phi_-(x) \alpha^{2L-x} \right], \quad (6)$$

with  $0 < |\alpha| < 1$  being the parameter which fully characterizes the individual states and  $N$  a normalization factor. The Bloch functions  $\phi_{+(-)}(x)$  correspond to those associated with  $\alpha$  ( $\alpha^{-1}$ ). These Bloch functions can be obtained using Bloch's theorem, i.e., by considering the local Schrödinger equation for each site in the unit cell and individually taking an ansatz of either  $\phi_+(x)\alpha^x$  or  $\phi_-(x)\alpha^{-x}$  then using  $\phi_\pm(x) = \phi_\pm(x + \tau)$  so that the Bloch functions are obtained after solving  $\tau - 1$  linear coupled equations. Note, in the course of solving for the Bloch functions we will also obtain the analytical form of the energy spectrum  $E(\alpha)$ . The normalization factor for each state can be calculated using the Bloch functions and the quantized values of  $\alpha$  as

$$N = \left[ \sum_{x=x_0+1}^{L-1} \left| \phi_+(x) \alpha^x - \frac{\phi_+(L)}{\phi_-(L)} \phi_-(x) \alpha^{2L-x} \right|^2 \right]^{-1/2}. \quad (7)$$

The quantization of  $\alpha$  to give a finite number of states is dependent on the boundary condition and the form of the Hamiltonian. We can solve for  $\alpha$  in two ways, either by taking the general quantization condition given by the boundary conditions  $\psi(x_0) = \psi(L) = 0$  to obtain

$$\alpha^{2(L-x_0)} = \frac{\phi_+(x_0)\phi_-(L)}{\phi_+(L)\phi_-(x_0)}, \quad (8)$$

or by considering the Schrödinger equation at a single site, we will consider it at site  $x_0 + 1$  and use  $\psi(x_0) = 0$  to obtain

$$E(\alpha) = J_{x_0+1} \frac{\psi(x_0 + 2)}{\psi(x_0 + 1)} + \mu_{x_0+1}. \quad (9)$$

When solving for a bound state in the system we will need to solve the local Schrödinger equation given by Eq. (9), as the presence of a bound state does not solely rely on the boundary conditions which is what leads us to the quantization condition of Eq. (8).

States contained within energy bands and not within band gaps are described in terms of plane waves with real quasimomentum  $k$ . This means that a number of the solutions obtained from the above equations will be of the form  $\alpha = e^{ik}$  and if no in-gap states are present, then all the solutions will be of this form. It is worth noting that for a commensurate system  $\phi_\pm(x_0) = \phi_\pm(L)$ , we can solve for the quasimomenta for any Hamiltonian without even defining the Hamiltonian, as the quantization condition of Eq. (8) in this case is  $e^{2i(L-x_0)k} = 1$ ,

which has known solutions of

$$k = \frac{\pi n}{L - x_0}, \quad (10)$$

with  $n \in \mathbb{Z}$  being the quantum number that characterizes the different eigenstates. The fixed quasimomenta of commensurate lattices will allow us to simplify the CD terms for them substantially, as we will outline below.

Note that while for a general tight-binding model with a defined unit cell, any present edge states will be in gap. It is possible to have other in-gap states which are not due to the topology or on the edge, e.g., states bound to a defect [36,47]. In this work, we will use the terms in-gap state and edge state interchangeably but note here that the general solution given in Eq. (6) and, therefore, the derived counterdiabatic terms of Sec. IV, can be applied to other in-gap bound states.

We do not make any assumption on whether the creation and annihilation operators of Hamiltonian (4) obey commutation or anticommutation relations, but consider the solutions for a single-particle which are given by Eq. (6). From these, the noninteracting picture can be developed for many particles, if it is of interest, for either bosonic or fermionic systems.

## IV. EXACT COUNTERDIABATIC DRIVING IN LATTICES

### A. All states

To write the counterdiabatic terms of noninteracting lattice models we first need to outline the construction of the operator summed over in Eq. (3). The eigenstates of general 1D lattice models are given by Eq. (5) with the wave function  $\psi_\alpha(x)$  given in Eq. (6). Using these, we can then take the derivative with respect to  $\lambda$  to obtain

$$\partial_\lambda \psi_\alpha(x) = N \left[ \phi_+(x) \alpha^x A_\alpha(x) - \frac{\phi_+(L)}{\phi_-(L)} \phi_-(x) \alpha^{2L-x} B_\alpha(x) \right], \quad (11)$$

where we have defined

$$A_\alpha(x) = \frac{\partial_\lambda N}{N} + \frac{\partial_\lambda \phi_+(x)}{\phi_+(x)} + x \frac{\partial_\lambda \alpha}{\alpha} \quad (12)$$

and

$$B_\alpha(x) = \frac{\partial_\lambda N}{N} + \frac{\partial_\lambda \phi_+(L)}{\phi_+(L)} - \frac{\partial_\lambda \phi_-(L)}{\phi_-(L)} + \frac{\partial_\lambda \phi_-(x)}{\phi_-(x)} + (2L - x) \frac{\partial_\lambda \alpha}{\alpha}. \quad (13)$$

We will now outline how each term for  $A_\alpha(x)$  and  $B_\alpha(x)$  can be analytically obtained. First, the terms which are derivatives of Bloch functions can be obtained after these are solved for in a given model. We will discuss this for an the example in Sec. V and can not go further here without knowing the form of the Bloch functions.

Next, we consider the term  $\partial_\lambda N$ , which we can write as

$$\partial_\lambda N = -\frac{1}{2} N^3 \sum_{x=x_0+1}^{L-1} [\tilde{\psi}_\alpha^*(x) \partial_\lambda \tilde{\psi}_\alpha(x) + \tilde{\psi}_\alpha(x) \partial_\lambda \tilde{\psi}_\alpha^*(x)], \quad (14)$$

with  $\tilde{\psi}_\alpha(x) = \psi_\alpha(x)/N$ , i.e., the wave function without normalization. The derivative of the unnormalized wave

functions can be written out as

$$\partial_\lambda \tilde{\psi}_\alpha(x) = \phi_+(x) \alpha^x \tilde{A}_\alpha(x) - \frac{\phi_+(L)}{\phi_-(L)} \phi_-(x) \alpha^{2L-x} \tilde{B}_\alpha(x), \quad (15)$$

with

$$\tilde{A}_\alpha(x) = A_\alpha(x) - \frac{\partial_\lambda N}{N} \quad (16)$$

and

$$\tilde{B}_\alpha(x) = B_\alpha(x) - \frac{\partial_\lambda N}{N}. \quad (17)$$

Finally, we are left with the term proportional to  $\partial_\lambda \alpha$ . For commensurate systems where the quasimomentum of the bulk states is well defined by  $k = n\pi/(L - x_0)$  (see Sec. III), the term  $\partial_\lambda \alpha$  will be zero for all states within the bulk energy bands. This is because for these states  $\alpha = e^{ik}$  and the quasimomentum is entirely defined from the boundary conditions. Note, in this case, the  $\partial_\lambda N$  is also zero, and we can simplify the expressions for  $A_\alpha(x)$  and  $B_\alpha(x)$  considerably to only rely on the Bloch functions. This still leaves us with needing to know  $\partial_\lambda \alpha$  for in-gap states or for bulk states in incommensurate lattices. We can obtain this by differentiating the local Schrödinger equation of Eq. (9) with respect to  $\lambda$ . Once we know  $\alpha$  we can then simply substitute this in and rearrange this new differentiated local Schrödinger equation to analytically obtain  $\partial_\lambda \alpha$ .

We can now write the form of the additional CD term to counter transitions between all instantaneous eigenstates as

$$H_{\text{CD}} = i \sum_\alpha \sum_{x, x'=x_0+1}^{L-1} \theta_\alpha(x, x') b_x^\dagger b_{x'}, \quad (18)$$

where the summation runs over both  $x$  and  $x'$  such that the CD term couples all sites in the chain. The strength of this coupling is described by the function

$$\theta_\alpha(x, x') = |N|^2 \psi_\alpha^*(x') \left[ \phi_+(x) \alpha^x A_\alpha(x) - \frac{\phi_+(L)}{\phi_-(L)} \phi_-(x) \alpha^{2L-x} B_\alpha(x) \right]. \quad (19)$$

### B. Targeted states

In certain situations, e.g., in ground-state coherent quantum annealing, we will only be interested in staying in one single state of the system and it is desirable to only counter the diabatic terms out of this target state. We propose that this targeted CD can be realized by the addition of terms of the form

$$H_{\text{CD}}^\alpha = i |\partial_\lambda \psi_\alpha(x)\rangle \langle \psi_\alpha(x)| - i |\psi_\alpha(x)\rangle \langle \partial_\lambda \psi_\alpha(x)|. \quad (20)$$

Similar forms for CD of particular states have been considered previously [48–50], especially when trying to reduce the energetic overhead for implementation. We can then write this for noninteracting lattice models as

$$H_{\text{CD}}^\alpha = i \sum_{x, x'=x_0+1}^{L-1} [\theta_\alpha(x, x') b_x^\dagger b_{x'} - \theta_\alpha^*(x, x') b_{x'}^\dagger b_x], \quad (21)$$

with  $\alpha$  being that of the targeted state, e.g., the instantaneous ground state for coherent quantum annealing. We will see in the example of Sec. V that the targeted CD term can result in a simplification of the control terms that need to be implemented.

### C. Properties of the general counterdiabatic driving terms

Having derived the general forms of the CD for all states and targeted at a particular state we can briefly discuss the implications of their general form.

First, the counterdiabatic terms are not limited to the nearest-neighbor tunneling restriction of the Hamiltonian considered. They instead couple through tunneling between all sites. The coupling between sites is reminiscent of density-dependent tunneling, which would be the only term of the extended tight-binding model relevant to a noninteracting system. However, in this case, the density-dependent tunneling is required in a “mean-field way,” with it not being dependent on the density in the new counterdiabatic Hamiltonian but the density in the original Hamiltonian.

The form of the long-range tunneling of the CD is then dependent on  $\theta_\alpha(x, x')$  given in Eq. (19). To understand this term we can ignore the normalization constant  $|N|^2$ , which is only a constant prefactor. The conjugate state  $\psi_\alpha^*(x')$ , which is the density on the site corresponding to the annihilation operator, is an envelope function. As a result,  $\theta_\alpha(x, x')$  for each state with a corresponding  $\alpha$  will be bounded by the form of the state.

The key detailed features of the CD are then contained in the functions  $A_\alpha(x)$  and  $B_\alpha(x)$ . For the context of this discussion it will be sufficient to consider one of these functions  $A_\alpha(x)$  given by Eq. (11), with the other sharing similar terms. We can first note that the derivative of the normalization term is reliant on the other terms in  $A_\alpha(x)$ , as seen in Eqs. (14)–(17). The next term in  $A_\alpha(x)$  is dependent on the derivative of the Bloch functions, which itself will be periodic up to  $\tau$ . However, the final term is proportional to  $x$  which breaks the periodicity of the Hamiltonian. As a result, the long-range tunneling of the CD,  $\theta_\alpha(x, x')$ , will not in general be periodic with the same periodicity as the Hamiltonian.

Note, for the case of periodic boundary conditions the analytical state is given by  $\psi_\alpha^{\text{PB}}(x) = N \phi_+(x) \alpha^x$ , i.e., the first term of the open boundary solution. In this case the CD term is equivalent to Eqs. (18) and (21) but with the condition that  $B_\alpha(x) = 0$  and  $\phi_-(x) = 0$ . Therefore, even for the case of periodic boundary conditions, where the states themselves are periodic with the periodicity  $\tau$ , the CD term will in general not be periodic due to the final term of  $A_\alpha(x)$ .

However, there is a central case where this linear term in  $x$  is not present, and that is the commensurate case of  $\phi_\pm(x) = \phi_\pm(x + \tau)$  considered in detail in the example below. In this case, if there are not any in-gap states then  $\partial_\lambda \alpha = 0$  for all states and the term proportional to  $x$  plays no role. However, if there are edge states present in the spectrum of a commensurate lattice, then for these states alone  $\partial_\lambda \alpha \neq 0$ , and we will get a contribution from the term proportional to

$x$  with a constant prefactor, or slope, dependent on  $\alpha$ , which itself is not  $x$  dependent.

## V. STATE TRANSFER IN THE TOPOLOGICAL SU-SCHRIEFFER-HEEGER MODEL

### A. Su-Schrieffer-Heeger model

As an example, we will consider adiabatic state transfer through the topological edge states of a one-dimensional model, the Su-Schrieffer-Heeger (SSH) model. The SSH model was first introduced as a model of polyacetylene [51] and has topological edge states with a corresponding nontrivial Zak's phase [52]. This model has been realized in ultracold atoms [53], the energy levels of a Rydberg atom [54], photonic lattices [55–57], and acoustic waveguides [58]. There has been particular interest in studying topologically protected state transfer in the SSH model and the optimization of such a transfer, including removing the requirement for adiabatic evolution [37–45]. Recently, edge-to-edge state transfer was experimentally demonstrated using a synthetic lattice of up to 10 sites constructed from the momentum states of ultracold atoms [59].

The SSH model has no onsite potential and has nearest-neighbor tunneling which alternates in strength, meaning we can write the Hamiltonian as

$$H(\lambda) = J \sum_{x=x_0+1}^{L-1} [[1 - \lambda(-1)^x]b_x^\dagger b_{x+1} + \text{H.c.}], \quad (22)$$

with  $2\lambda$  being the difference in strength between the alternating tunneling and  $J$  the tunneling strength which will set the units of energy. Note that time will therefore be given in units of  $J^{-1}$ . We will consider a commensurate finite system, i.e.,  $\phi_\pm(L) = \phi_\pm(x_0)$ . For the commensurate lattice, we can perform a state transfer between the two edges of the system by initializing the system on the  $x_0 + 1$  edge with a large  $\lambda_0$  then driving the system towards  $-\lambda_0$ . If the sweep through  $\lambda$  is performed adiabatically, the final result will be the perfect transfer of the state to the  $L - 1$  edge. This state transfer protocol is illustrated in Fig. 1, including examples of the edge state for different  $\lambda$ .

Using the approach outlined in Sec. III, the spectrum

$$E_{s,\alpha} = (-1)^s \sqrt{\left(\frac{1+\alpha^2}{\alpha}\right)^2 - \lambda^2 \left(\frac{\alpha^2-1}{\alpha}\right)^2}, \quad (23)$$

with  $s = 0, 1$  labeling the two bands, and Bloch functions

$$\phi_+(x) = \left( \frac{1}{\frac{(1+\alpha^2)-\lambda(1-\alpha^2)}{E_{s,\alpha}}} \right), \quad (24)$$

can be found, which is represented in the standard form of a two-component vector with each component corresponding to that for each of the two sites in the unit cell. To obtain  $\phi_-(x)$  we implement the transformation  $\alpha \rightarrow 1/\alpha$  to Eq. (24). Note that as would be expected,  $E_{s,\alpha} \equiv E_{s,1/\alpha}$ .

The spectrum for a commensurate system with  $\phi_\pm(L) = \phi_\pm(x_0)$ , i.e., for the SSH model  $L - x_0 = 2m$  with  $m \in \mathbb{Z}$ , as a

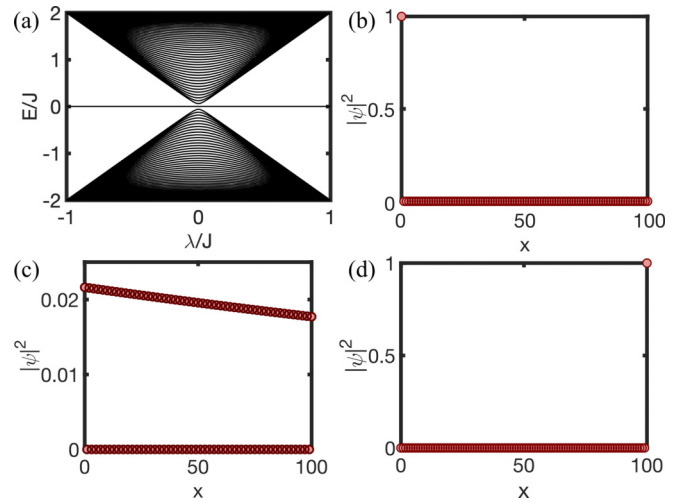


FIG. 1. Spectrum and edge states of the SSH model given by Hamiltonian (22) using the analytical energy and states for a system of 101 sites. (a) The spectrum of all states for each individual  $\lambda/J$  as given by Eq. (23) with the states in the bulk having  $\alpha = e^{ik}$  with a quasimomentum  $k = \pi n/102$ , with  $n \in \mathbb{Z}$  starting at one and monotonically increasing for each state, and the in-gap edge state being described by an  $\alpha$  obtained by solving the Schrödinger equation at the first site. We show the probability density for (b) the in-gap state at  $\lambda/J = 0.999$  with  $\alpha = 0.0224e^{i\pi/2}$  and occupation on only even sites, (c) the in-gap state at  $\lambda/J = 10^{-3}$  with  $\alpha = 0.999e^{i\pi/2}$ , and (d) the in-gap state at  $\lambda/J = -0.999$  with  $\alpha = 0.0224e^{i\pi/2}$ .

function of  $\lambda$  is shown in Fig. 1(a) for  $x_0 = -1$  and  $L = 101$ . We already know all the solutions in the two bulk bands, as the quantization condition for commensurate systems enforces  $k = \pi n/(L - x_0)$ . For finite  $\lambda$  there are two bands, as there are two sites in the unit cell. This means we only need to solve for the missing state which is in the band gap, this can be done by solving the local Schrödinger equation of Eq. (9) for  $\alpha$ . Note, this will give us all of the bulk solutions as well, but the problem can be simplified as we know the quasimomentum must be that of the missing state  $k = \pi/2$  [36]. This means we can take  $\alpha = ae^{i\pi/2}$  where  $a \in \mathbb{R}$  and solve Eq. (9) for  $a$ , giving us a single solution, that of the in-gap edge state. Note, at  $\lambda = 0$  we return to a single-band model and  $a = 1$ . With positive  $\lambda$  the edge state will be bound to the  $x_0$  site boundary and for negative  $\lambda$  to the  $L$  site boundary, with examples shown in Figs. 1(b) and 1(d). Therefore, if we follow the in-gap state adiabatically from positive to negative  $\lambda$  in a dynamical protocol, we will transfer a particle from one edge to the other.

However, there is an issue in realizing this adiabatic protocol, the gap closes at  $\lambda = 0$  as can be seen in Fig. 1(a) and from the fact that  $a = 1$  at this point, i.e., the solution is that of a bulk state in a band. To be adiabatic one would need to drive slowly through this region, with a rate of change of the parameter being inversely proportional to the gap between the state we desire to remain in and the nearest other eigenstate. As we approach  $\lambda = 0$ , the edge state begins to stretch further into the system, as is shown for  $\lambda/J = 10^{-3}$  in Fig. 1(c). In this example, we will use the approaches outlined in Sec. IV to study the diabatic terms that arise from the closing of this

gap and what is needed to implement perfect state transfer in arbitrary time.

For the SSH model, we can confirm the gap goes to zero for large  $L$  (and fixed  $x_0$ ) and obtain its scaling. As we are working with a commensurate system  $\phi_{\pm}(L) = \phi_{\pm}(x_0)$ , we know the quasimomenta for all of the bulk states and we know that the edge state has  $k = \pi/\tau$ . Using the fact that the edge state will have zero energy and that the spectrum is symmetric, we can calculate the gap simply by looking at the energy of the previous state which will have quantum number  $n = (L-1)/2$  for the commensurate case and therefore  $k = \pi(L-1)/2(L-x_0)$ . Fixing  $x_0 = -1$  we find the gap is given by

$$\Delta E(\lambda) = \sqrt{2} \sqrt{1 + \lambda^2 + (1 - \lambda^2) \cos\left(\frac{(L-1)\pi}{L+1}\right)}, \quad (25)$$

which has  $\lim_{L \rightarrow \infty} \Delta E(\lambda) = 2\lambda$ , as  $\lim_{L \rightarrow \infty} \frac{L-1}{L+1} = 1$ .

A protocol of edge-to-edge transfer can also be realized for the incommensurate case of  $\phi_{\pm}(L) \neq \phi_{\pm}(x_0)$ , which is only true for  $L - x_0 = 2m + 1$  with  $m \in \mathbb{Z}$ . This is the case for which the bulk-boundary correspondence [31] can be applied and there is a topological phase transition at  $\lambda = 0$  characterized by Zak's phase [52], with two degenerate edge states for  $\lambda > 0$  and no edge states for  $\lambda \leq 0$ . The protocol to implement the edge-to-edge transfer in the incommensurate case relies on the degeneracy of the edge states and does not cross the topological phase transition where the gap closes [60]. In this sense, the protocol for the commensurate case is more interesting from a counterdiabatic driving perspective, with the requirement that the gap-closing point is traversed. Note that the gap closing for the commensurate case is not a topological phase transition, with one edge state present in the spectrum on either side of this point.

## B. Counterdiabatic driving

In constructing the CD terms, we know that the derivatives of the Bloch functions with respect to the varying parameter play a vital role. For the SSH model, we can find these by differentiating Eq. (24) and obtain

$$\partial_{\lambda} \phi_{+}(x) = \frac{1}{E_{s,\alpha}} \begin{pmatrix} 0 \\ \frac{1-\alpha^4-4\lambda\alpha\partial_{\lambda}\alpha}{(\lambda-1)\alpha^3-(1+\lambda)\alpha} \end{pmatrix} \quad (26)$$

and

$$\partial_{\lambda} \phi_{-}(x) = \frac{1}{E_{s,\alpha}} \begin{pmatrix} 0 \\ \frac{1-\alpha^4-4\lambda\alpha\partial_{\lambda}\alpha}{(1+\lambda)\alpha^3-(1-\lambda)\alpha} \end{pmatrix}. \quad (27)$$

By differentiating the local Schrödinger equation of Eq. (9) for this example, we can also obtain for the in-gap states that

$$\partial_{\lambda} \alpha = -\alpha \frac{1 + 2\alpha^2 + \alpha^4 + \lambda^3 - 2\alpha^2\lambda^3 + \alpha^4\lambda^3}{\lambda(\alpha^4 - 1)(\lambda - 1)(1 + \lambda)^2}. \quad (28)$$

Note, the bulk states of a commensurate lattice have  $\partial_{\lambda} \alpha = 0$  as discussed in Sec. IV.

### 1. All states

First, we will consider the normal form of CD, which includes the corrections for all instantaneous eigenstates. The

form of CD for all states for noninteracting lattice models is given in Eq. (18), and is fully characterized for each potential hopping term between  $x$  and  $x'$  by

$$\Theta(x, x') = \sum_{\alpha} \theta_{\alpha}(x, x'). \quad (29)$$

We will consider the state transfer protocol in the SSH model by initializing a system at  $\lambda_0 = 0.9$  in the in-gap state then linearly driving  $\lambda$  to  $\lambda_f = -0.9$  thus transferring the state from the left to the right edge of the system as is shown in Fig. 1. Imposing the evolution of the system under  $H + H_{\text{CD}}$ , with  $H_{\text{CD}}$  given in Eq. (18), we obtain unit fidelity state transfer across the lattice for all total driving times and system sizes.

We show the strength of the tunneling terms between all  $x$  and  $x'$  in the upper triangles of Fig. 2, the operator is Hermitian so symmetric up to a local phase around  $x = x'$ . Two examples are shown for a small and large lattice with 11 and 101 sites, respectively, and we find that the form of the CD term is very similar through various commensurate system sizes. We find that as we approach the gap-closing point, the tunneling terms required to enforce CD become longer in range, reflecting the more delocalized nature of the state at this point [see Fig. 1(c)]. We repeat here that implementation of the full modified Hamiltonian  $H + H_{\text{CD}}$  with the form of  $H_{\text{CD}}$  given by the upper triangles of Fig. 2 results in unit fidelity state transfer in arbitrary time.

### 2. Targeted state

We now consider the case of CD for only a single state as described by Eq. (21), which is particularly useful in this state preparation scenario where we desire to remain in a single instantaneous eigenstate of the system. We can characterize the strength of the tunneling simply with  $\theta_{\alpha}(x, x')$  with  $\alpha$  corresponding to the state of interest, in this case the in-gap state. Imposing the evolution of the system under  $H + H_{\text{CD}}^{\alpha}$ , with  $H_{\text{CD}}^{\alpha}$  given in Eq. (21), we again obtain unit fidelity state transfer across the lattice for all total driving times and system sizes.

We show the strength of the tunneling terms in order to enforce CD for the in-gap state in the lower triangles of Fig. 2, for systems of size 11 and 101. Again, the operator is Hermitian so symmetric up to a local phase around  $x = x'$ . A number of differences to the full CD terms are immediately observed. First, at large  $|\lambda|$  the CD terms to correct for diabatic excitations away from the in-gap state only require tuning the tunneling coefficients near the edge that is populated. While this may be easier to realize in a given physical setup, as it does not require tuning all tunneling coefficients at all ranges, it creates an overall aperiodic Hamiltonian. This should not be a surprise to us, as the in-gap edge states are inherently asymmetric, as they are bound to a particular edge. When  $|\lambda|$  is decreased, we observe again that longer-range tunnelings come into play. However, this does not become as uniform as in the case of the full CD with the longest tunneling terms dominating as we approach  $\lambda = 0$ .

### 3. Properties and dynamics

We first note here that the difference between the large- $\lambda$  CD terms of Fig. 2(a) and the small- $\lambda$  CD terms of Fig. 2(d)

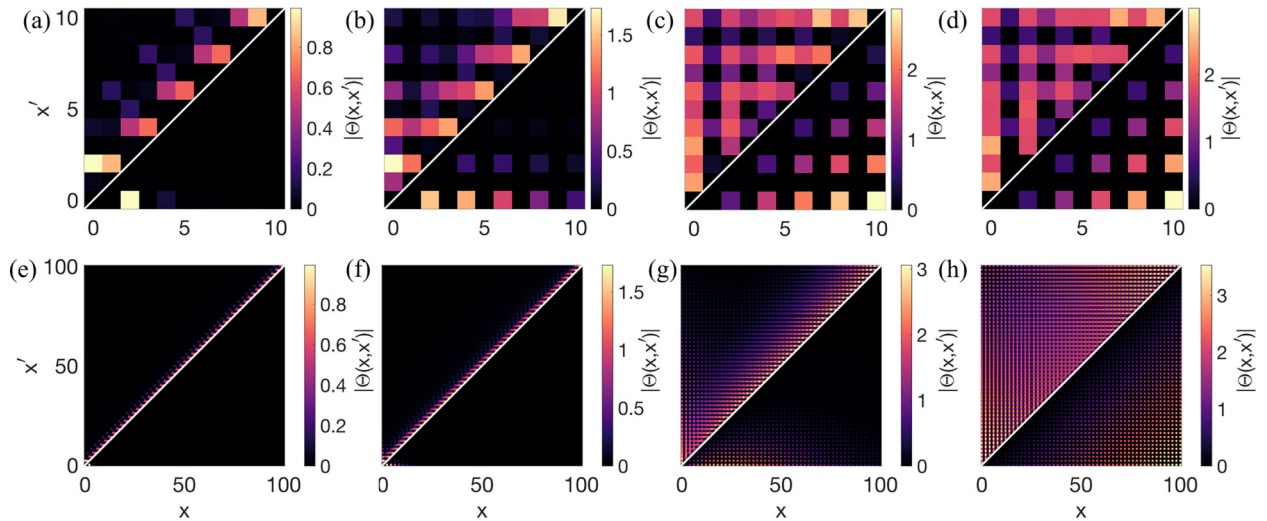


FIG. 2. Examples of the form of the CD terms through plots of the absolute value in each element of the matrix of the CD term for the same driving as considered in Fig. 5. The CD terms are Hermitian and each image shows the form of the full CD term  $H_{\text{CD}}$  in the upper triangle and the targeted CD term  $H_{\text{CD}}^{\alpha}$  using only the in-gap state in the lower triangle. Note that diagonal terms are trivially zero for CD and we have separated the triangles with a white line. We consider two different system sizes (a)–(d) 11 and (e)–(h) 101 sites as well as a number of different points along the driving with (a), (e)  $\lambda/J = 0.9$ , (b), (f)  $\lambda/J = 0.36$ , (c), (g)  $\lambda/J = 4.6 \times 10^{-2}$ , and (d), (h)  $\lambda/J = 10^{-3}$ .

give an example of the discussion in Sec. IV C of the physical implications that can be seen from the analytical equations, i.e., when an edge state is present the CD terms will have a contribution from a term linear in  $x$ , this is shown in Fig. 2(a), as the CD terms are stronger on one side of the lattice than on the other. Whereas, for the case of weak  $\lambda$ , where the influence of the edge state will be minor, we can observe that the CD terms are symmetric around the center of the lattice and it is the term linear in  $x$  is playing a minor role.

It is known that the norm of a CD term can be sensitive to points where energy gaps close [14,27,61,62]; this is a particular issue if there is only one gap present in the system. We plot the Euclidean norm of the CD terms for both the full CD and targeted CD in Fig. 3(a) for 101 sites and confirm that it does diverge around the gap-closing point. Note that in any finite system, this divergence will appear finite as we will have a small but finite gap between the states.

From the forms of the CD given in Fig. 2, it is clear that a key feature is that as we decrease  $\lambda$  towards zero, we populate the diagonals further away from the central diagonal of  $\theta_{\alpha}(x, x')$  or  $\Theta(x, x')$  with nonzero entries. In other words, long-range tunnelings become increasingly important. In Figs. 3(b)–3(d), we plot the ratio of the norm of the CD terms including up to  $d$  diagonals below the central diagonal, with all other values set to zero, and the norm of the CD term for three different  $\lambda$  values. The ratio of norms for the case of large  $|\lambda|$  is shown in Fig. 3(b) with both the full and targeted CD described by only a few diagonals as would be expected from the local nature of the CD tunneling shown in Fig. 2(e). When  $|\lambda|$  is decreased, as is shown in Figs. 3(c) and 3(d), the CD terms become more nonlocal in nature and begin to be dominated by terms that are longer in range.

The impact of the highly nonlocal CD terms in the final achieved state transfer fidelity is shown for both the targeted

and full CD approaches in Fig. 4. Across both approaches, it is clear in Fig. 4 that the nonlocal terms are crucial to the transfer of the state, as would be expected, as the gap closing at  $\lambda = 0$  will have a significant impact on the diabatic transitions during the protocol.

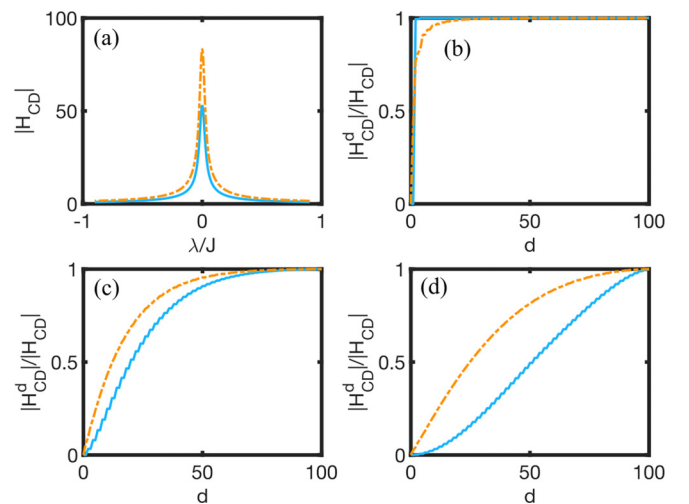


FIG. 3. The norm of the CD terms in the SSH model for the same example as shown in Fig. 2 for 101 sites. Protocol is from  $\lambda/J = 0.9$  to  $-0.9$  in a total time of  $\tau J = 1$ . We show the case of all CD terms given by  $H_{\text{CD}}$  as dashed-dotted (orange) lines and the targeted CD terms given by  $H_{\text{CD}}^{\alpha}$  using only the in-gap state as a solid (blue) line. (a) Shows the Euclidean norm of the CD terms as a function of  $\lambda/J$ , showing a clear increase in the “strength” of the CD terms around the gap-closing point of  $\lambda/J = 0$ . (b)–(d) Show the percentage of the Euclidean norm that is accounted for when including  $d$  diagonals of the matrix at (b)  $\lambda/J = 0.9$ , (c)  $\lambda/J = 0.046$ , and (d)  $\lambda/J = 10^{-3}$ , with all of  $H_{\text{CD}}$  being accounted for at 100 diagonals.

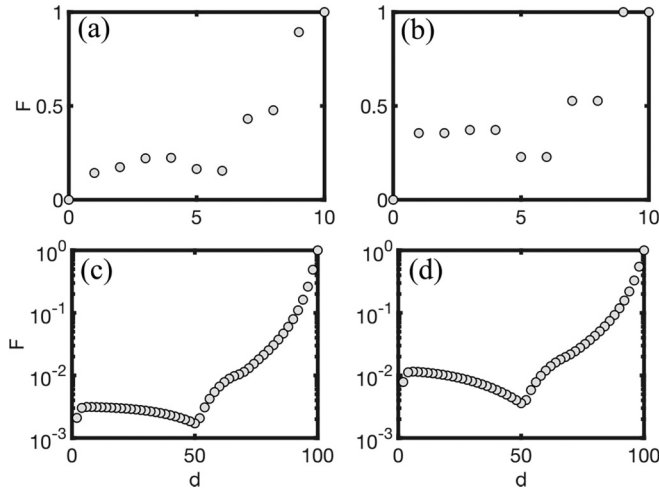


FIG. 4. The state transfer fidelity after implementing CD including up to  $d$  diagonals of the CD Hamiltonian for the same protocol as in Fig. 3. (a), (b) Show the case of 11 sites and (c), (d) 101 sites with (a) and (c) being the implementation of all CD terms given by  $H_{CD}$  and (b) and (d) the targeted CD terms given by  $H_{CD}^\alpha$  using only the in-gap state. The state transfer fidelity after implementation of the bare protocol with no CD is  $F = 10^{-10}$  for 11 sites and  $F < 10^{-14}$  for 101 sites.

### C. Spectra of the modified counterdiabatic Hamiltonian

Given that we have obtained the full analytical CD terms, we can also consider the spectra of the modified Hamiltonians under which we evolve when we add CD, given by  $H(\lambda) + H_{CD}(\lambda)$ . We plot these in Fig. 5 for the case of 11 and 101 sites and the driving protocol considered so far. We solve for both the full and targeted CD using the analytical approach outlined in Sec. IV but numerically solve for the instantaneous eigenstates corresponding to  $H(\lambda) + H_{CD}(\lambda)$ , as the modified Hamiltonian can be aperiodic and non-sparse, due to the asymmetric form of the CD Hamiltonian, as is shown in Fig. 2. The analytical approach can still be applied in this regime but is rather inefficient in this scenario as it will require  $\tau = L - x_0$  nonlocal coupled Schrödinger equations to be solved, especially around the gap-closing point.

The impact of the inclusion of CD terms targeted at a particular state is clear for the case of 11 sites in Fig. 5(b) as the result is that an increased minimal gap has been opened between the state at energy zero and the neighboring states, with this gap being  $\Delta E/J = 0.261$  before the addition of the CD term for the in-gap state and  $\Delta E/J = 1$  with the CD term. Note that we can calculate the minimal gap without the CD term from Eq. (25). When we go to a larger system of 101 sites [Figs. 5(e) and 5(f)], it does not immediately look like the minimal gap has been made larger as, of course, all of the eigenstates are far closer. However, in this case, we again see that the gap has been increased from  $\Delta E/J = 0.031$  without CD to  $\Delta E/J = 0.124$  with the inclusion of CD terms for the in-gap state. Note, in order to open this gap in each case the CD terms impose a penalty in energy (away from zero) for some states, resulting in states being pushed out the top and bottom of the bands around  $\lambda/J = 0$ . For larger systems, this penalty appears more severe, and it is this that we observe as

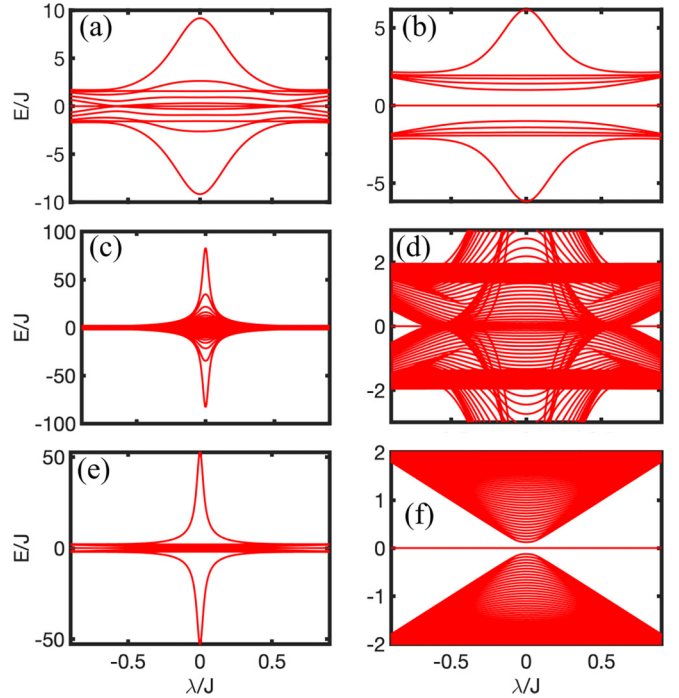


FIG. 5. Examples of the spectrum of the full Hamiltonian with CD for both (a), (c), (d) the full CD term so the Hamiltonian is  $H(\lambda) + H_{CD}(\lambda)$  and (b), (e), (f) the targeted CD term for the in-gap state so the Hamiltonian is  $H(\lambda) + H_{CD}^\alpha(\lambda)$ . Examples are shown for a total drive time of  $\tau J = 1$  for systems of size (a), (b) 11 sites and (c)–(f) 101 sites. The plots in (d) and (f) are zoomed-in portions of (c) and (e), respectively, to see the spectrum around the central  $E/J = 0$  state. The CD terms are found using the analytical approach outlined in Sec. IV and the eigenvalue problem is solved numerically.

a divergence in the norm of the CD terms at the gap-closing point in Fig. 3(a).

In Fig. 6 we consider the scaling of the gap for a small finite  $\lambda/J = 1.8 \times 10^{-3}$  for both the original Hamiltonian and the Hamiltonian with targeted CD. We observe that the

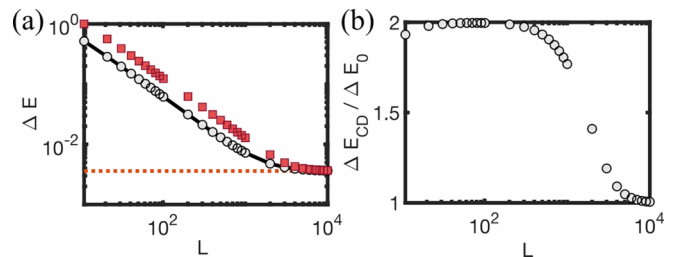


FIG. 6. Scaling of the gap near the topological transition  $\lambda/J = 1.8 \times 10^{-3}$ . (a) The scaling of the energy gap between the zero-energy topological edge state and the nearest state in energy. The analytical energy gap, given by Eq. (25), is shown by a solid (black) line which is in agreement with the numerical gap for the SSH model with Hamiltonian (22) by circles (gray). The gap for the CD Hamiltonian of the targeted approach, shown in Figs. 5(b) and 5(f), is given by squares (red). We also plot the limit  $\lim_{L \rightarrow \infty} \Delta E(\lambda) = 2\lambda$  by a dotted (red) line. (b) The ratio of the gap of the CD Hamiltonian targeting the edge state  $\Delta E_{CD}$  to the analytical energy gap  $\Delta E_0$  of the SSH model.

gap obtained from numerical diagonalization for the original Hamiltonian  $H(\lambda)$  is in agreement with the analytical form derived earlier [see Eq. (25)], and that it converges to the infinite-size limit of  $2\lambda$ . We observe that the energy gap for the Hamiltonian with targeted CD,  $H(\lambda) + H_{\text{CD}}^\alpha(\lambda)$ , is a factor of 2 larger than the energy gap in the nonmodified Hamiltonian, before eventually also converging to the infinite-size limit value of  $2\lambda$ .

The spectra for the modified Hamiltonian for the full CD term are shown in Figs. 5(a) for 11 sites and 5(c) and 5(d) for 101 sites. There are similarities between these and the spectra of the targeted CD terms, mainly states being pushed out to energies far from zero, resulting in a similar behavior of the norm. It is clear though that the spectrum of this modified Hamiltonian is far more complex and it is difficult to build an understanding of how this modified Hamiltonian imposes the adiabatic approximation in arbitrary time from its spectra alone. It is clear that the full CD term is not opening a gap for the edge state. We know this is not necessary as the eigenstates of the modified Hamiltonian are not required to be equivalent to or bear any resemblance with the eigenstates of the bare Hamiltonian with no CD. Further study of the connection between the eigenstates of the CD and bare Hamiltonians could provide insight into the key requirements for developing fast protocols for more complex settings.

## VI. CONCLUSION AND OUTLOOK

In this work, we have extended the set of known examples where the exact analytical form of CD can be found to include the general Hamiltonian of noninteracting particles, which can be either bosons or fermions, in 1D lattices. We built upon previous work [36] that outlined the analytical states for both bulk and edge states to construct the CD terms exactly. We outlined how this approach can be applied to general problems in this family of Hamiltonians and derived expressions for terms that appear in the CD. We also discussed a targeted approach for countering transitions out of a particular state.

As an example, we considered the CD terms, both for all states and targeted at a particular state, for state transfer in the topological SSH model. The approach developed enabled us to study the properties of the CD terms for large systems with no penalty due to the size of the system. Note that while the Hilbert space is only increasing linearly with system size, the analytical approach outlined can still outperform numerically obtaining the eigenstates, especially for the commensurate case. We restricted the shown results to a lattice of 101 sites as

this allowed for the behavior of large systems to be observed clearly in the plots, and the CD terms can be obtained analytically for arbitrarily large system sizes.

The approach outlined in this work could also be extended to higher-dimensional systems with open boundaries that can be reduced to one-dimensional models, e.g., crystalline models in cylindrical geometries. It could also be extended to study few-body systems where the wave functions can be written as combinations of the noninteracting states, or the CD terms obtained here could be used as starting points for control functions in many-body systems for variational CD approaches [18,21].

The requirement to control terms over arbitrarily long distances will be a common feature of CD terms in lattices, as the CD operator is generated by a term proportional to  $|\partial_\lambda \psi_n(\lambda)\rangle \langle \psi_n(\lambda)|$ . We observed this in the noninteracting case for the tunneling terms in the SSH model, especially as we approached the point where the band gap closed. For the many-body case, it is highly likely that exact CD will require the full extended Hubbard [63] or Bose-Hubbard model [64] to be controlled, i.e., long-range tunneling, interaction, pair tunneling, and density-dependent tunneling terms. It is possible to engineer the terms of the extended Bose-Hubbard model, including long-range tunneling, through placing ultracold atoms in optical lattices in a cavity [65–67]. While it is possible that such an approach could in principle realize the CD terms of this work, it is unlikely that the structure of the exact CD terms discussed here could be easily engineered.

However, knowledge of the exact CD terms provides us with additional information about the dynamics of a quantum system outside of the adiabatic approximation. For example, the adiabatic gauge potential, which for a choice of gauge is equivalent to the CD Hamiltonian up to a global phase, has been utilized as a numerically efficient cost function for optimal control protocols [21], to define and probe the properties of chaotic behavior [61,68], to probe the presence of quantum phase transitions [27,62], and, in general, to study nonequilibrium behavior [20].

The data for this manuscript is available in open access at [69].

## ACKNOWLEDGMENTS

The author thanks A. J. Daley, E. D. C. Lawrence, S. Morawetz, and C. Hickey for helpful discussions. This work was supported by the Engineering and Physical Sciences Research Council through Grant No. EP/Y005058/2.

- 
- [1] D. Aharonov, W. Van Dam, J. Kempe, Z. Landau, S. Lloyd, and O. Regev, Adiabatic quantum computation is equivalent to standard quantum computation, *SIAM Rev.* **50**, 755 (2008).
  - [2] T. Albash and D. A. Lidar, Adiabatic quantum computation, *Rev. Mod. Phys.* **90**, 015002 (2018).
  - [3] R. D. Somma, D. Nagaj, and M. Kieferová, Quantum speedup by quantum annealing, *Phys. Rev. Lett.* **109**, 050501 (2012).
  - [4] A. Rajak, S. Suzuki, A. Dutta, and B. K. Chakrabarti, Quantum annealing: An overview, *Phil. Trans. R. Soc. A.* **381**, 20210417 (2023).
  - [5] M. Born and V. Fock, Beweis des adiabatensatzes, *Z. Phys.* **51**, 165 (1928).
  - [6] T. Kato, On the adiabatic theorem of quantum mechanics, *J. Phys. Soc. Jpn.* **5**, 435 (1950).
  - [7] S. Jansen, M.-B. Ruskai, and R. Seiler, Bounds for the adiabatic approximation with applications to quantum computation, *J. Math. Phys.* **48**, 102111 (2007).
  - [8] S. J. Glaser, U. Boscain, T. Calarco, C. P. Koch, W. Köckenberger, R. Kosloff, I. Kuprov, B. Luy, S. Schirmer, T. Schulte-Herbrüggen *et al.*, Training schrödinger's cat: Quantum

- optimal control: Strategic report on current status, visions and goals for research in europe, *Eur. Phys. J. D* **69**, 279 (2015).
- [9] J. Werschnik and E. Gross, Quantum optimal control theory, *J. Phys. B: At. Mol. Opt. Phys.* **40**, R175 (2007).
- [10] D. Guéry-Odelin, A. Ruschhaupt, A. Kiely, E. Torrontegui, S. Martínez-Garaot, and J. G. Muga, Shortcuts to adiabaticity: Concepts, methods, and applications, *Rev. Mod. Phys.* **91**, 045001 (2019).
- [11] E. Torrontegui, S. Ibáñez, S. Martínez-Garaot, M. Modugno, A. del Campo, D. Guéry-Odelin, A. Ruschhaupt, X. Chen, and J. G. Muga, Shortcuts to adiabaticity, in *Advances in Atomic, Molecular, and Optical Physics*, Vol. 62 (Elsevier, Amsterdam, 2013), pp. 117–169.
- [12] M. Demirplak and S. A. Rice, Adiabatic population transfer with control fields, *J. Phys. Chem. A* **107**, 9937 (2003).
- [13] M. Demirplak and S. A. Rice, Assisted adiabatic passage revisited, *J. Phys. Chem. B* **109**, 6838 (2005).
- [14] M. V. Berry, Transitionless quantum driving, *J. Phys. A: Math. Theor.* **42**, 365303 (2009).
- [15] A. del Campo, Shortcuts to adiabaticity by counterdiabatic driving, *Phys. Rev. Lett.* **111**, 100502 (2013).
- [16] A. del Campo, M. M. Rams, and W. H. Zurek, Assisted finite-rate adiabatic passage across a quantum critical point: Exact solution for the quantum Ising model, *Phys. Rev. Lett.* **109**, 115703 (2012).
- [17] B. Damski, Counterdiabatic driving of the quantum Ising model, *J. Stat. Mech.* (2014) P12019.
- [18] D. Sels and A. Polkovnikov, Minimizing irreversible losses in quantum systems by local counterdiabatic driving, *Proc. Natl. Acad. Sci. USA* **114**, E3909 (2017).
- [19] P. W. Claeys, M. Pandey, D. Sels, and A. Polkovnikov, Floquet-engineering counterdiabatic protocols in quantum many-body systems, *Phys. Rev. Lett.* **123**, 090602 (2019).
- [20] M. Kolodrubetz, D. Sels, P. Mehta, and A. Polkovnikov, Geometry and non-adiabatic response in quantum and classical systems, *Phys. Rep.* **697**, 1 (2017).
- [21] I. Čepaitė, A. Polkovnikov, A. J. Daley, and C. W. Duncan, Counterdiabatic optimized local driving, *PRX Quantum* **4**, 010312 (2023).
- [22] J. Yao, L. Lin, and M. Bukov, Reinforcement learning for many-body ground-state preparation inspired by counterdiabatic driving, *Phys. Rev. X* **11**, 031070 (2021).
- [23] E. J. Meier, K. Ngan, D. Sels, and B. Gadway, Counterdiabatic control of transport in a synthetic tight-binding lattice, *Phys. Rev. Res.* **2**, 043201 (2020).
- [24] Q. Xie, K. Seki, and S. Yunoki, Variational counterdiabatic driving of the Hubbard model for ground-state preparation, *Phys. Rev. B* **106**, 155153 (2022).
- [25] F. P. Barone, O. Kiss, M. Grossi, S. Vallecorsa, and A. Mandarino, Counterdiabatic optimized driving in quantum phase sensitive models, *New J. Phys.* **26**, 033031 (2024).
- [26] K. Takahashi and A. del Campo, Shortcuts to adiabaticity in Krylov space, *Phys. Rev. X* **14**, 011032 (2024).
- [27] E. D. C. Lawrence, S. Schmid, I. Čepaitė, P. Kirton, and C. W. Duncan, Numerical approaches for non-adiabatic terms in quantum dynamics, [arXiv:2401.10985](https://arxiv.org/abs/2401.10985).
- [28] M. Z. Hasan and C. L. Kane, *Colloquium*: Topological insulators, *Rev. Mod. Phys.* **82**, 3045 (2010).
- [29] X.-L. Qi and S.-C. Zhang, Topological insulators and superconductors, *Rev. Mod. Phys.* **83**, 1057 (2011).
- [30] S. Rachel, Interacting topological insulators: a review, *Rep. Prog. Phys.* **81**, 116501 (2018).
- [31] J. K. Asbóth, L. Oroszlány, and A. Pályi, A short course on topological insulators, *Lect. Notes Phys.* **919**, 166 (2016).
- [32] Y. Hatsugai, Chern number and edge states in the integer quantum Hall effect, *Phys. Rev. Lett.* **71**, 3697 (1993).
- [33] D. Hügél and B. Paredes, Chiral ladders and the edges of quantum Hall insulators, *Phys. Rev. A* **89**, 023619 (2014).
- [34] I. C. Fulga, F. Hassler, and A. R. Akhmerov, Scattering theory of topological insulators and superconductors, *Phys. Rev. B* **85**, 165409 (2012).
- [35] J. Arkininstall, M. H. Teimourpour, L. Feng, R. El-Ganainy, and H. Schomerus, Topological tight-binding models from nontrivial square roots, *Phys. Rev. B* **95**, 165109 (2017).
- [36] C. W. Duncan, P. Öhberg, and M. Valiente, Exact edge, bulk, and bound states of finite topological systems, *Phys. Rev. B* **97**, 195439 (2018).
- [37] L. Qi, G.-L. Wang, S. Liu, S. Zhang, and H.-F. Wang, Engineering the topological state transfer and topological beam splitter in an even-sized Su-Schrieffer-Heeger chain, *Phys. Rev. A* **102**, 022404 (2020).
- [38] F. Mei, G. Chen, L. Tian, S.-L. Zhu, and S. Jia, Robust quantum state transfer via topological edge states in superconducting qubit chains, *Phys. Rev. A* **98**, 012331 (2018).
- [39] S. Longhi, G. L. Giorgi, and R. Zambrini, Landau-Zener topological quantum state transfer, *Adv. Quantum Technol.* **2**, 1800090 (2019).
- [40] N. E. Palaiodimopoulos, I. Brouzos, F. K. Diakonov, and G. Theocharis, Fast and robust quantum state transfer via a topological chain, *Phys. Rev. A* **103**, 052409 (2021).
- [41] F. M. D’Angelis, F. A. Pinheiro, D. Guéry-Odelin, S. Longhi, and F. Impens, Fast and robust quantum state transfer in a topological Su-Schrieffer-Heeger chain with next-to-nearest-neighbor interactions, *Phys. Rev. Res.* **2**, 033475 (2020).
- [42] L. Qi, G.-L. Wang, S. Liu, S. Zhang, and H.-F. Wang, Controllable photonic and phononic topological state transfers in a small optomechanical lattice, *Opt. Lett.* **45**, 2018 (2020).
- [43] C. Wang, L. Li, J. Gong, and Y.-X. Liu, Arbitrary entangled state transfer via a topological qubit chain, *Phys. Rev. A* **106**, 052411 (2022).
- [44] J. Zurita, C. E. Creffield, and G. Platero, Fast quantum transfer mediated by topological domain walls, *Quantum* **7**, 1043 (2023).
- [45] S. V. Romero, X. Chen, G. Platero, and Y. Ban, Optimizing edge-state transfer in a Su-Schrieffer-Heeger chain via hybrid analog-digital strategies, *Phys. Rev. Appl.* **21**, 034033 (2024).
- [46] M. V. Berry, Quantal phase factors accompanying adiabatic changes, *Proc. R. Soc. London A* **392**, 45 (1984).
- [47] W. Shockley, On the surface states associated with a periodic potential, *Phys. Rev.* **56**, 317 (1939).
- [48] M. Demirplak and S. A. Rice, On the consistency, extremal, and global properties of counterdiabatic fields, *J. Chem. Phys.* **129**, 154111 (2008).
- [49] Y. Zheng, S. Campbell, G. De Chiara, and D. Poletti, Cost of counterdiabatic driving and work output, *Phys. Rev. A* **94**, 042132 (2016).
- [50] S. Campbell, Quantum work statistics of controlled evolutions, *Europhys. Lett.* **143**, 68001 (2023).

- [51] W. P. Su, J. R. Schrieffer, and A. J. Heeger, Solitons in polyacetylene, *Phys. Rev. Lett.* **42**, 1698 (1979).
- [52] J. Zak, Berry's phase for energy bands in solids, *Phys. Rev. Lett.* **62**, 2747 (1989).
- [53] E. J. Meier, F. A. An, and B. Gadway, Observation of the topological soliton state in the Su–Schrieffer–Heeger model, *Nat. Commun.* **7**, 13986 (2016).
- [54] S. Kanungo, J. Whalen, Y. Lu, M. Yuan, S. Dasgupta, F. Dunning, K. Hazzard, and T. Killian, Realizing topological edge states with Rydberg-atom synthetic dimensions, *Nat. Commun.* **13**, 972 (2022).
- [55] N. Malkova, I. Hromada, X. Wang, G. Bryant, and Z. Chen, Observation of optical Shockley-like surface states in photonic superlattices, *Opt. Lett.* **34**, 1633 (2009).
- [56] P. St-Jean, V. Goblot, E. Galopin, A. Lemaître, T. Ozawa, L. Le Gratiet, I. Sagnes, J. Bloch, and A. Amo, Lasing in topological edge states of a one-dimensional lattice, *Nat. Photon.* **11**, 651 (2017).
- [57] S. Xia, D. Song, N. Wang, X. Liu, J. Ma, L. Tang, H. Buljan, and Z. Chen, Topological phenomena demonstrated in photorefractive photonic lattices, *Opt. Mater. Express* **11**, 1292 (2021).
- [58] A. Coutant, A. Sivadon, L. Zheng, V. Achilleos, O. Richoux, G. Theocharis, and V. Pagneux, Acoustic Su–Schrieffer–Heeger lattice: Direct mapping of acoustic waveguides to the Su–Schrieffer–Heeger model, *Phys. Rev. B* **103**, 224309 (2021).
- [59] T. Yuan, C. Zeng, Y.-Y. Mao, F.-F. Wu, Y.-J. Xie, W.-Z. Zhang, H.-N. Dai, Y.-A. Chen, and J.-W. Pan, Realizing robust edge-to-edge transport of atomic momentum states in a dynamically modulated synthetic lattice, *Phys. Rev. Res.* **5**, L032005 (2023).
- [60] N. Lang and H. P. Büchler, Topological networks for quantum communication between distant qubits, *npj Quantum Inf.* **3**, 47 (2017).
- [61] M. Pandey, P. W. Claeys, D. K. Campbell, A. Polkovnikov, and D. Sels, Adiabatic eigenstate deformations as a sensitive probe for quantum chaos, *Phys. Rev. X* **10**, 041017 (2020).
- [62] T. Hatomura and K. Takahashi, Controlling and exploring quantum systems by algebraic expression of adiabatic gauge potential, *Phys. Rev. A* **103**, 012220 (2021).
- [63] N. H. Le, A. J. Fisher, and E. Ginossar, Extended Hubbard model for mesoscopic transport in donor arrays in silicon, *Phys. Rev. B* **96**, 245406 (2017).
- [64] O. Dutta, M. Gajda, P. Hauke, M. Lewenstein, D.-S. Lühmann, B. A. Malomed, T. Sowiński, and J. Zakrzewski, Non-standard Hubbard models in optical lattices: a review, *Rep. Prog. Phys.* **78**, 066001 (2015).
- [65] H. Ritsch, P. Domokos, F. Brennecke, and T. Esslinger, Cold atoms in cavity-generated dynamical optical potentials, *Rev. Mod. Phys.* **85**, 553 (2013).
- [66] R. Landig, L. Hruby, N. Dogra, M. Landini, R. Mottl, T. Donner, and T. Esslinger, Quantum phases from competing short-and long-range interactions in an optical lattice, *Nature (London)* **532**, 476 (2016).
- [67] J. Argüello-Luengo, A. González-Tudela, T. Shi, P. Zoller, and J. I. Cirac, Analogue quantum chemistry simulation, *Nature (London)* **574**, 215 (2019).
- [68] C. Lim, K. Matirko, A. Polkovnikov, and M. O. Flynn, Defining classical and quantum chaos through adiabatic transformations, *arXiv:2401.01927*.
- [69] C. Duncan, Data for: “Exact counterdiabatic driving in finite topological lattice models”, University of Strathclyde, (12 June 2024), <https://doi.org/10.15129/e78ec94b-967f-4df5-b488-b5a6482e8b91>.